Available online at www.sciencedirect.com

ScienceDirect

Journal of Nutritional Biochemistry 155 (2026) 110372

Journal of Nutritional Biochemistry

RESEARCH PAPER

Small litter size attenuates adverse hepatic effects induced by a high-sucrose diet

Juliana Letícia Silva[a,b], Isabela Jesus de Deus[a,b], Aline Rezende Ribeiro de Abreu[a,b], Miliane Martins de Andrade Fagundes[a,b], Gustavo Silveira Breguez[d], Cláudia Martins Carneiro[e], Sílvia Paula-Gomes[f], Daniela Caldeira Costa[g], Karina Barbosa de Queiroz[a,b,c,*]

[a] Experimental Nutrition Laboratory, Department of Food Science, School of Nutrition, Federal University of Ouro Preto (Universidade Federal de Ouro Preto), Ouro Preto, Minas Gerais, Brazil
[b] Graduate Program in Health and Nutrition, School of Nutrition, Federal University of Ouro Preto (Universidade Federal de Ouro Preto), Ouro Preto, Minas Gerais, Brazil
[c] Brazilian National Institute of Science and Technology for DOHaD (INCT-DOHaD), Brazil
[d] Multiuser Laboratory for Research in Nutritional Biochemistry and Molecular Biology, School of Nutrition, Federal University of Ouro Preto (Universidade Federal de Ouro Preto), Ouro Preto, Minas Gerais, Brazil
[e] Immunopathology Laboratory, Center for Research in Biological Sciences, Federal University of Ouro Preto (Universidade Federal de Ouro Preto), Ouro Preto, Minas Gerais, Brazil
[f] Biochemistry and Molecular Biology Laboratory, Department of Biological Sciences, Federal University of Ouro Preto (Universidade Federal de Ouro Preto), Ouro Preto, Minas Gerais, Brazil
[g] Metabolic Biochemistry Laboratory, Department of Biological Sciences, Institute of Biological Sciences, Federal University of Ouro Preto (Universidade Federal de Ouro Preto), Ouro Preto, Minas Gerais, Brazil

Received 15 October 2025; received in revised form 26 March 2026; accepted 6 April 2026

Abstract

We evaluated whether metabolic imprinting (MI) induced by small litter size (SL) could mitigate liver damage, redox imbalance, and NLR family pyrin domain-containing 3 (NLRP3) inflammasome activation caused by a high-sucrose diet (HSD) in young rats. Male Wistar rats (P0) were divided into control litters (CL; 8 pups/dam) and SLs (4 pups/dam). After weaning, they were fed for 8 weeks with a standard diet (STD) or HSD (30% sucrose), and distributed into four groups: STD-CL, HSD-CL, STD-SL, and HSD-SL. After euthanasia, blood and liver samples were collected for analysis. The HSD impaired hepatic insulin signaling and promoted hepatic alterations associated with NLRP3 inflammasome activation. Although the HSD increased antioxidant enzyme activity, it also altered the nonalcoholic fatty liver disease activity score (NAS) and elevated oxidative damage. SL-induced MI attenuated oxidative stress, as evidenced by reduced p47phox(Ser359) expression and decreased hepatic protein and lipid oxidation, potentially modulating the interaction between the experimental variables and p-AKT(Ser473). In addition, SL attenuated NLRP3 inflammasome activation and decreased caspase-1 and IL-18 levels. This study provides novel evidence that SL-induced MI attenuates adverse hepatic changes, oxidative stress, and NLRP3 inflammasome activation promoted by HSD. Our findings not only challenge the current literature but also suggest that SL-induced metabolic plasticity enables adaptations to post-weaning dietary variations, thereby mitigating hepatic damage induced by a post-weaning HSD in young rats.

Keywords: DOHaD; Litter size effect; High-sucrose diet; Oxidative stress; NLRP3 inflammasome; p47phox.

1. Introduction

Metabolic imprinting (MI) is the process by which environmental factors, particularly nutritional exposure during critical developmental windows, induce long-lasting phenotypic changes via epigenetic mechanisms [1,2]. This concept underlies the Developmental Origins of Health and Disease (DOHaD) hypothesis, which proposes that early-life exposure can shape health trajectories and influence disease susceptibility across the lifespan [3,4]. Understanding the timing and nature of early nutritional influences, as well as their ability to modulate epigenetic pathways, is crucial for elucidating the mechanisms of MI and guiding effective preventive strategies.

From this perspective, exclusive breastfeeding on demand is considered the gold standard for infant nutrition during the first 6 months of life, followed by the introduction of appropriate complementary feeding [5]. Within nutrition, excessive intake of sugars, particularly sucrose, during this critical developmental window and throughout childhood has been associated with an increased risk of obesity, dyslipidemia, type 2 diabetes, and

* Corresponding author at: Federal University of Ouro Preto, Rua Dois, Campus Morro do Cruzeiro - Bauxita, Ouro Preto, CEP 35400-000, Brazil.
E-mail address: karina.queiroz@ufop.edu.br (K.B. de Queiroz).

https://doi.org/10.1016/j.jnutbio.2026.110372

metabolic dysfunction-associated steatotic liver disease (MASLD) [6,7].

In experimental models, chronic exposure to a high-sucrose diet (HSD) promotes *de novo* lipogenesis, hepatic lipid accumulation, and mitochondrial dysfunction, which enhance reactive oxygen species (ROS) production and activate inflammatory pathways that contribute to insulin resistance (IR) and liver injury [8,9]. In turn, ROS can influence redox-sensitive signaling, partly through NADPH oxidase (NOX) activation, particularly via phosphorylation of the p47phox subunit at Ser 359 and/or Ser 370 [10,11].

The pathophysiology of IR is closely linked to chronic low-grade inflammation mediated by the innate immune responses [12]. Excess ROS also provides the second signal required for NLRP3 inflammasome activation, promoting IL-1β and IL-18 maturation, thereby impairing insulin signaling in the liver, notably by reducing the phosphorylation of p-AKT(Ser 473) [13,14]. Despite these advances, the precise contributions of NOX-driven oxidative stress and NLRP3 activation to hepatic IR following HSD consumption remain poorly defined.

The small litter size (SL) model, in which 2-4 pups are reared per dam instead of 6-12 pups, has been widely employed to investigate MI. SL offspring typically display increased adiposity, dyslipidemia, glucose intolerance, and IR later in life [15–17]. However, emerging evidence has suggested that the SL model may confer adaptive responses, including neuroprotection and resilience to diet-induced inflammation [18,19]. These heterogeneous findings indicate that the SL model can modulate metabolic plasticity; however, its interaction with post-weaning dietary challenges and hepatic inflammatory mechanisms is not well understood.

Importantly, although SL has been linked to oxidative imbalance and inflammatory changes [20,21], little is known about its impact on hepatic NLRP3 inflammasome activation and NOX regulation. Previous work has shown that fructose can promote hepatic NLRP3 activation via oxidative stress and increased NOX activity [22], though another study reported IR and NF-κB increase without detectable changes in NLRP3 protein expression, suggesting that this pathway may not always participate in fructose-induced hepatic inflammation [23]. We recently demonstrated that SL enhanced metabolic plasticity and mitigated systemic IR induced by a post-weaning HSD [24]. SL offspring exhibited increased body mass at weaning compared to control litter animals (59.05±8.32 g *vs.* 53.65±3.03 g, respectively). Following HSD exposure, caloric intake was increased, while the diet promoted adiposity expansion and alterations in circulating triacylglycerol (TAG) levels in both litter groups. Notably, despite systemic IR induced by a post-weaning HSD, SL animals displayed attenuation of key glycometabolic disturbances, including reduced serum TAG and insulin levels, lower HOMA-IR, and enhanced brown adipose tissue activation, effects accompanied by reduced oxidative damage [24]. In light of these findings, this model combined with post-weaning HSD is a valuable tool to investigate hepatic responses to early-life nutritional programming and IR.

Therefore, the present study investigated whether SL-induced MI alters liver injury, redox imbalance, and NLRP3 inflammasome activation induced by post-weaning HSD exposure in young rats. Special attention was paid to p47phox phosphorylation at Ser359, a key step in hepatic NOX activation, and its potential role in linking ROS generation to NLRP3 inflammasome-mediated hepatic IR. Although our findings challenge the current literature, they indicate that SL-induced MI enhances adaptive responses to post-weaning dietary challenges and mitigates liver damage induced by a post-weaning HSD in young rats, highlighting the potential role of early life programming in protecting against diet-driven hepatic damage.

2. Materials and methods

2.1. Ethics statement, animals, and diet

All animal procedures were approved by the Ethics Committee for the Use of Animals at the Federal University of Ouro Preto (protocol number: 2245040518). To evaluate litter–size effects, male Wistar rats were assigned to control litters (CL; 8 pups/dam) or SLs (4 pups/ dam), as described previously [25]. In rats, the lactation period lasts approximately 21 d (P0–P21), with young rats reaching approximately 8 weeks thereafter [26]. After weaning, offspring received one of two diets for 8 weeks: a standard commercial chow diet (STD, Nuvilab, Nuvital-CR, Colombo, Brazil) or a HSD (condensed milk 40.44%, crystal sugar 8.6%) and water (30% sucrose). The complete nutritional composition of the modified diet has been previously published and validated in our laboratory; macronutrient composition and energy density are shown in Table 1 [24].

2.2. Experimental design

Newborn male Wistar rats (P0; n=49) were pooled and randomly redistributed to foster dams to form either CL (8 pups/dam) or SL (4 pups/dam). Litter size manipulation was maintained throughout the lactation period (P0–P21) and used exclusively as a model of early-life nutritional programming at the Animal Science Center. After weaning (P21), pups were considered independent experimental units (*i.e.*, analyzed individually rather than as litters with their dams) and were randomly redistributed into four groups according to their post-weaning diet for 8 weeks: (1) STD-CL (n=11), (2) HSD-CL (n=13), (3) STD-SL (n=12), and (4) HSD-SL (n=13). Animals were housed under controlled conditions (12 h light/dark cycle, 24±2°C) with *ad libitum* access to food and water. The experimental model was previously established and validated as described elsewhere [24].

2.3. Euthanasia

After 8 weeks of dietary intervention, non-fasted animals were anesthetized with 5% isoflurane (Isoforine, São Paulo, Brazil) and euthanized by decapitation. Isoflurane was selected for its rapid onset and minimal discomfort and was used uniformly to avoid variability in accordance with ethical guidelines [27]. Blood was collected for serum analysis, and liver samples were either fixed for histology or stored at −80°C for later analysis.

2.4. Serum markers of liver damage

Serum was obtained by centrifugation and used to quantify liver damage markers using commercial kits according to the

Table 1
Macronutrient composition and energy density of the diets fed to rats for 8 weeks.

Macronutrient compound/100 g	STD	HSD
Kcal	310	313
Carbohydrates	46.75	55.91
Sucrose	NA	31.34
Humidity	10.61	20.04
Protein	20.72	12.13
Lipids	4.47	4.58

Abbreviations: HSD, high-sucrose diet; STD, standard diet.
Adapted by de Deus et al. (2025) [24].

manufacturer's instructions. Aspartate aminotransferase (AST; #52-200) and alanine aminotransferase (ALT; #53-200) were measured (Labtest Diagnóstica S.A. Minas Gerais, Brazil), and the absorbance was read at 500 nm. The results were expressed as U/mL.

2.5. Relative liver mass and characterization of the hepatic lipid profile

Relative liver mass was expressed as the ratio of liver weight to final body weight (g/g). The hepatic lipid content was determined using the Folch method [28]. Triacylglycerol (TAG; #87-2/100) and hepatic cholesterol (#76-2/100) concentrations were measured in lipids resuspended in isopropyl alcohol (Alphatec, Rio de Janeiro, Brazil) using commercial kits (Labtest Diagnóstica S. A.) according to the manufacturer's instructions. The absorbance was read at 505 nm, and the results were expressed as mg/dL.

2.6. Liver histomorphology

Liver sections were fixed for 72 h in a 20% dimethyl sulphoxide (Labsynth, São Paulo, Brazil) and 80% methanol (Alphatec) solution, with daily replacement. After the fixation process, tissues were embedded in paraffin, sectioned at 5 μm, and stained with hematoxylin-eosin. Sections per animal were analyzed under 40 × magnification using a Leica DM5000B microscope with LeicaQwin V3 software (Leica Microsystems, Wetzlar, Germany), and images from random fields were captured. Histological evaluation was performed according to the nonalcoholic fatty liver disease activity score (NAS), assessing hepatocellular ballooning (0=none, 1=few foci, 2=many foci), steatosis (0=<5%, 1=5–33%, 2=33–66%, 3=>66% of hepatocytes affected), and lobular inflammation (0=no foci, 1=1–2 foci, 2=3–4 foci, 3=>4 foci) [29,30].

2.7. Evaluation of the redox process: antioxidant enzymes and markers of oxidative damage

To assess redox process markers, liver samples were homogenized in phosphate buffer (1:10; 100 mM; pH 7.8) containing 1% protease inhibitor cocktail (#P8340; Sigma-Aldrich, St Louis, MO, USA). The total protein was quantified using Lowry's method [31]. Superoxide dismutase (SOD) activity was determined via the reduction of MTT [3-(4,5-dimethyl-thiazol 2-yl) 2,5-diphenyl tetrazolium bromide] by pyrogallic acid in alkaline medium (570 nm) [32,33], and catalase (CAT) activity by H_2O_2 decomposition using the Lambert-Beer law (240 nm) [34]. Both were expressed as U/mg protein. Sulfhydryl groups were measured using Ellman's reagent (DTNB [(5,5′-dithio-bis-(2-nitrobenzoic acid)]) at 412 nm and expressed as μmol/mg protein [35]. Oxidative damage markers included protein carbonyls (PCO), quantified via the 2,4-dinitrophenylhydrazine reaction (370 nm) [36], and malondialdehyde (MDA), measured using the thiobarbituric acid-reacting substances assay (532 nm) [37], both of which were expressed as nmol/mg protein.

2.8. Determination of protein expression by Western Blot: p-AKT(Ser473) and p47phox (Ser359)

The protein expression of p-AKT(Ser473) and p47phox (Ser359), was assessed by Western blotting analyses using rabbit-derived antibodies: anti-phospho-AKT (Ser473) (1:1000, #SAB4504331, Sigma-Aldrich), anti-AKT (1:1000, #SAB4500799, Sigma-Aldrich), anti-p47phox (1:500, #SAB4502810, Sigma-Aldrich), anti-p47-phospho (Ser359) (1:500, #SAB4504289, Sigma-Aldrich). Liver tissue (30 mg) was homogenized in RIPA buffer (50 mM Tris-HCl, pH 7.4), centrifuged at 12,000 × *g* for 40 min, and total protein was quantified using the Lowry method [31]. For analysis, 25 μg of total protein were separated on 10% SDS-PAGE gels and transferred to a nitrocellulose membrane in a Mini-Protean transfer system (Bio-Rad, Hercules, CA, USA). The membranes were blocked and incubated overnight with primary antibodies, followed by incubation with an anti-IgG secondary antibody (1:5000, #4414S, Cell Signaling Technology, Danvers, MA). Protein bands were detected via chemiluminescence, imaged, and quantified using the ImageJ software (http://rsb.info.nih.gov/ij/). Protein expression was normalized to total protein content assessed by Ponceau S staining after transfer. Densitometric analyses included all biological replicates from each group, whereas representative Western blot images depict a single sample per group. Band intensities were corrected to the total membrane signal, in accordance with Sander et al. [38]. Phosphorylated protein levels were expressed as the ratio of phosphorylated to total protein.

2.9. Gene expression of NLRP3 inflammasome components

The relative gene expression of the NLRP3 inflammasome components (*Nlrp3, Asc [pycard], Caspase-1, Il-1β, and Il-18)* was evaluated using the reverse transcription polymerase chain reaction and real-time quantification (RT-qPCR) technique. Liver samples (30 mg) were homogenized in Trizol (Invitrogen, Waltham, MA, USA), and RNA was extracted using chloroform (Sigma-Aldrich), purified with the SV Total RNA Isolation kit (#Z3105, Promega, Madison, WI, USA), and treated with DNAse I (Promega). RNA concentration and purity were verified by NanoDrop (Thermo Fisher Scientific, Waltham, MA, USA), with the 260/280 and the 260/230 ratios higher than 1.8 considered ideal. RNA integrity was confirmed using 1.2% agarose gel electrophoresis. Complementary DNA (cDNA) was synthesized from 1000 ng of total RNA using a High-Capacity cDNA RT kit (Thermo Fisher). Gene expression quantification was carried out using the SYBR Green system (Thermo Fisher) on the ABI 7500 Real-Time PCR System (Applied Biosystems, Foster City, CA, USA). Quantitative RT-PCR was performed using an initial step at 50°C for 2 min, followed by enzyme activation at 95°C for 10 min and 40 amplification cycles (95°C for 15 s 60°C for 1 min). Melting curve analysis with continuous fluorescence acquisition was performed to confirm amplification specificity (95°C for 15 s; 60°C for 1 min; 95°C for 30 s and 60°C for 15 s). Primers were designed using the *Primer Design Tool* software (https://www.ncbi.nlm.nih.gov/tools/primer-blast/), and sequences are shown in Table 2. Primer efficiency and specificity were validated by melting curve analysis. Gene expression was normalized to *B2m* and calculated using the $2^{-\Delta Cq}$ method [39].

2.10. Activation of the NLRP3 inflammasome

To evaluate hepatic inflammasome activation, the caspase-1 enzymatic activity and IL-18 concentration were quantified using commercial kits. Liver protein extracts were prepared in PBS, and the supernatant was obtained by centrifugation. Protein concentrations were determined by the Lowry method [31]. Caspase-1 activity was measured using the Caspase 1 Activity Assay Kit *(Colorimetric Method)* (#E-CK-A381; Elabscience, Houston, TX, USA), following the manufacturer's instructions. This method is based on the cleavage of the AC-YVAD-pNA substrate and absorbance readings at 405 nm, with the results expressed in U/mg protein. The concentration of IL-18 was determined by chemiluminescence ELISA using the commercial Rat IL-18 (Interleukin 18) CLIA Kit (#E-CL-R0401, Elabscience) and was expressed in pg/mL.

Table 2
Primer sequences and characteristics used for RT-qPCR.

Gene	ID	Primer	Tm	%CG
Nlrp3	NM_001191642.1	F: 5'GGCGAGACCTCTGGGAAAAA3'	54	55
		R: 5'CTGTCTTCCTGGCACACCAT3'	54	55
Asc	NM_172322.2	F: 5'CACTCATTGCCAGGGTCACA 3'	54	55
		R: 5'CACGAACTGCCTGGTACTGT3'	54	55
Caspase-1	NM_012762.3	F: 5'GACCGAGTGGTTCCCTCAAG3'	54	60
		R: 5'GACGTGTACGAGTGGGTGTT3'	54	55
Il-1β	NM_031512.2	F: 5'ACCTATGTCTTGCCCGTGGA3'	55	55
		R: 5'TCGTCATCATCCCACGAGTC3'	54	55
Il-18	NM_019165.2	F: 5'AAGAAACCCGCCTGTGTTCG3'	55	55
		R: 5'GGTCACAGCCAGTCCTCTTA3'	53	55
B2m	NM_012512.2	F: 5'CGGTGACCGTGATCTTTCTGG3'	55	57
		R: 5'CGGTGGATGGCGAGAGTACA3'	56	60

Abbreviations: Asc, apoptosis-associated speck-like protein containing a CARD domain; B2m, Beta-2-microglobulin; %CG: cytosine - guanine content (%); Il-1B, interleukin-1 beta; Il-18, interleukin-18; ID, primer identifier; Nlrp3, NLR family pyrin domain-containing 3 receptor; Tm, melting temperature (°C).

2.11. Statistical analysis

Statistical analyses were performed using the GraphPad Prism software (version 9; GraphPad Software Inc., Irvine, CA, USA). Sample size (up to 13 animals/ group) was calculated based on the Lee Index to ensure statistical power of 0.9 ($\alpha = 0.05$). Data normality was assessed using the Shapiro–Wilk test. Parametric data were expressed as mean ± standard deviation (SD), whereas non-parametric data (NAS score) were expressed as median and interquartile range (IQR). Two-way analysis of variance (ANOVA) was used to evaluate the effects of the interaction between litter size and post-weaning diet, followed by the Bonferroni *post hoc* test when appropriate. In the absence of interactions, the main effects were analyzed independently using the Mann–Whitney U test. Outliers were identified using the interquartile range method. Correlations were assessed using Spearman's test. For nonparametric data (NAS score), comparisons among groups were performed using the Kruskal–Wallis test followed by Dunn's multiple comparisons test. $P<.05$ was considered statistically significant.

3. Results

3.1. HSD induces hepatic damage and lipid accumulation after 8 weeks

The results are shown in Figure 1. The post-weaning diet significantly influenced the liver enzyme activity ($P<.05$). *Post hoc* analysis demonstrated a significant difference between the HSD-CL and STD-CL, while no other pairwise comparisons reached statistical significance. ALT levels increased by approximately 50% in the HSD-CL group (59.16±22.42) compared to the levels observed in the STD-CL group (38.57±8.09) (Fig. 1A). Importantly, no differences were observed between the HSD-CL and HSD-SL groups, indicating that this effect is primarily driven by the post-weaning diet and occurs independently of litter size. Similarly, AST activity was affected by the post-weaning diet ($P<.05$), increasing ~50% in the HSD-CL group (181.3±52.50) relative to the STD-CL group (121.3±29.22). No differences were detected between HSD-CL and HSD-SL groups, reinforcing that the observed changes are attributable to diet rather than litter size (Fig. 1B). No significant differences were observed in relative liver weight (Fig. 1C). In contrast, hepatic lipid content was significantly affected by the post-weaning diet ($P<.05$). The *post hoc* analysis indicated a difference between HSD-CL and STD-CL groups, with no additional pairwise differences. A 3.4-fold increase was observed in the HSD-CL group compared to the STD-CL group (Fig. 1D). Notably, no differences were observed between the HSD-CL and HSD-SL groups, indicating that lipid accumulation is driven by the post-weaning diet independently of litter size. The hepatic triacylglycerol levels were also influenced by the post-weaning diet ($P<.001$) (Fig. 1E), with a post hoc analysis showing an increase in the HSD-CL group (45.94±10.78 *vs.* 22.67±9.78) and HSD-SL groups (41.23±5.9 *vs.* 30.1±5.9) compared to their respective controls. No differences were observed between HSD-CL and HSD-SL groups, further supporting that these effects are primarily driven by the post-weaning diet rather than litter size. Conversely, hepatic cholesterol content was influenced by litter size and the interaction ($P<.05$) (Fig. 1E). Notably, cholesterol levels increased by ~100% in the STD-SL group (7.86±2.84) and ~90% in the HSD-CL group (7.22±2.40), when compared to the STD-CL group (3.75±2.02) (Fig. 1F).

3.2. SL mitigates hepatic histomorphological alterations induced by HSD after 8 weeks

Liver histomorphology was assessed using the NAFLD activity score (NAS), as shown in Figure 2. Although none of the groups reached an NAS ≥5, which characterizes NAFLD, significant differences were observed in total scores. Significant differences in NAS score were detected by the Kruskal–Wallis test ($P<.001$), with Dunn's post hoc analysis showing higher values in the HSD-CL group compared to STD-CL ($P<.001$) (Fig. 2B). Hepatocellular ballooning (Fig. 2C) showed a similar pattern ($P<.005$), as did liver inflammation (Fig. 2E; $P<.05$), both exhibiting higher values in HSD-CL compared to STD-CL. In contrast, steatosis (Fig. 2D) did not differ between groups, with hepatocyte involvement ranging from 5 to 33% in HSD animals. These alterations observed in HSD-CL were not observed in HSD-SL animals

3.3. SL attenuates hepatic oxidative damage induced by HSD after 8 weeks

To assess oxidative processes in the liver, we analyzed the activity of endogenous antioxidant enzymes (SOD and CAT), sulfhydryl group concentrations, and oxidative damage markers (PCO and MDA levels). SOD activity (Fig. 3A) was significantly affected by the interaction between SL size and post-weaning diet ($P<.05$), with a ~30% reduction in the HSD-SL group (1.46±0.30) compared to the STD-SL (2.14±0.58), and ~28% compared to the HSD-CL (2.04±0.38). A similar pattern was observed for CAT activ-

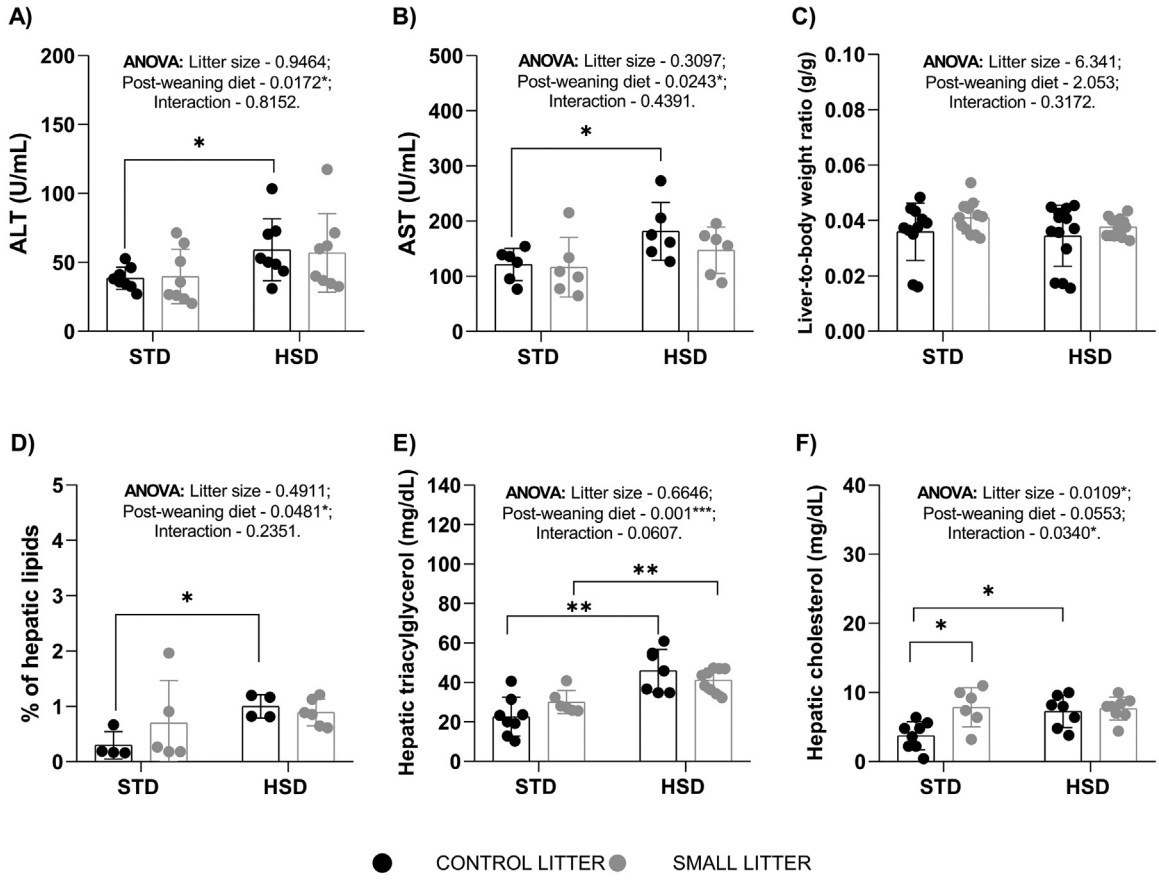

Fig. 1. HSD induces hepatic damage and the lipid accumulation after 8 weeks. (A) Alanine aminotransferase (ALT); U/mL (STD-CL=6); (STD-SL=6); (HSD-CL=6); (HSD-SL=6). (B) Aspartate aminotransferase (AST); U/mL (STD-CL=8); (STD-SL=8); (HSD-CL=8); (HSD-SL=8). (C) Liver-to-body weight ratio, g/g (STD-CL=11); (HSD-CL=13); (STD-SL=12); (HSD-SL=13). (D) Percentage of hepatic lipids (STD-CL=4); (HSD-CL=4); (STD-SL=5); (HSD-SL=6). (E) Hepatic triacylglycerol; mg/dL (STD-CL=8); (HSD-CL=7); (STD-SL=6); (HSD-SL=9). (F) Hepatic cholesterol; mg/dL (STD-CL=8); (HSD-CL=7); (STD-SL=6); (HSD-SL=8). Data normality was assessed using the Shapiro–Wilk test. Parametric data are represented as mean ±SD and are represented using bar graphs, whereas nonparametric data are presented as median with interquartile range (IQR) and are illustrated with box plots. Pups were analyzed individually as independent experimental units. The effects of litter size and post-weaning diet were assessed by two-way ANOVA, followed by the Bonferroni *post hoc* test when interaction was observed. To evaluate the main effects independently (litter size and/or post-weaning diet), *post hoc* mean comparison tests were conducted to identify specific differences between the groups. CL, control litter; HSD, high-sucrose diet; SL, small litter; STD, standard diet. $^{*}P<.05$; $^{**}P<.01$; $^{***}P<.001$.

ity (Fig. 3B), which was influenced by the interactions between these factors ($P<.05$). The HSD-SL group exhibited a significant decrease of ~35% (179.5 ± 42.81) relative to both the STD-SL group (275.3±101.0) and the HSD-CL group (281.9±77.47). Regarding nonenzymatic antioxidant capacity, the concentration of sulfhydryl groups (Fig. 3F) was reduced by the post-weaning diet ($P<.05$), with a ~30% decrease in the HSD-SL group (56421±15294) compared to STD-SL (78990±19117).

Among the oxidative damage markers, the PCO levels (Fig. 3D) were significantly affected by the interaction between the variables ($P<.05$). The HSD-CL group showed a ~40% increase (2.64±0.57) compared to the STD-CL group (1.83±0.47), while the HSD-SL group presented a ~30% reduction (1.90±0.44) relative to HSD-CL. Similarly, MDA levels (Fig. 3E) were elevated in the HSD-CL group by ~45% (0.25±0.06) compared to STD-CL (0.17 ± 0.032), and were reduced by ~35% in the HSD-SL group (0.16±0.04) in comparison to HSD-CL group.

3.4. SL mitigates p47phox (Ser359) phosphorylation induced by HSD associated with oxidative damage and reveals an interaction effect on p-AKT (Ser473) expression

Given the link between the redox process, NOX activation, and hepatic IR, we assessed NOX complex activation through phosphorylation of the p47phox subunit at Ser359 [p47phox (Ser359)] and phosphorylation of AKT at Ser473 [p-AKT(Ser473)]. As shown in Figure 4, p47phox (Ser359) phosphorylation (Fig. 4A) was influenced by litter size ($P<.05$) and the interaction between the variables ($P<.05$). HSD markedly increased phosphorylation in the control group (HSD-CL: 2.19±0.75), representing a 100% rise compared to STD-CL (1.10±0.70). However, this increase was significantly attenuated in the HSD-SL group (0.60±0.70), showing a ~72.5% reduction relative to HSD-CL. p-AKT(Ser473) (Fig. 4B) was influenced by the interaction between variables (litter size and post-weaning diet) ($P<.05$), although no significant differences were detected among groups in the post hoc analysis.

3.5. SL attenuates caspase-1 activation induced by HSD and reduces IL-18 levels

In order to investigate the role of the NLRP3 inflammasome in our experimental conditions, we analyzed the hepatic expression of genes encoding key components of the oligomeric complex [*Nlrp3, Asc (Pycard), Caspase-1, Il-1β, and Il-18*] using reverse transcription polymerase chain reaction and real-time quantification. Additionally, inflammasome activation was assessed based on caspase-1 enzymatic activity and hepatic IL-18 concentration. These findings are presented in Figures 5 and 6, respec-

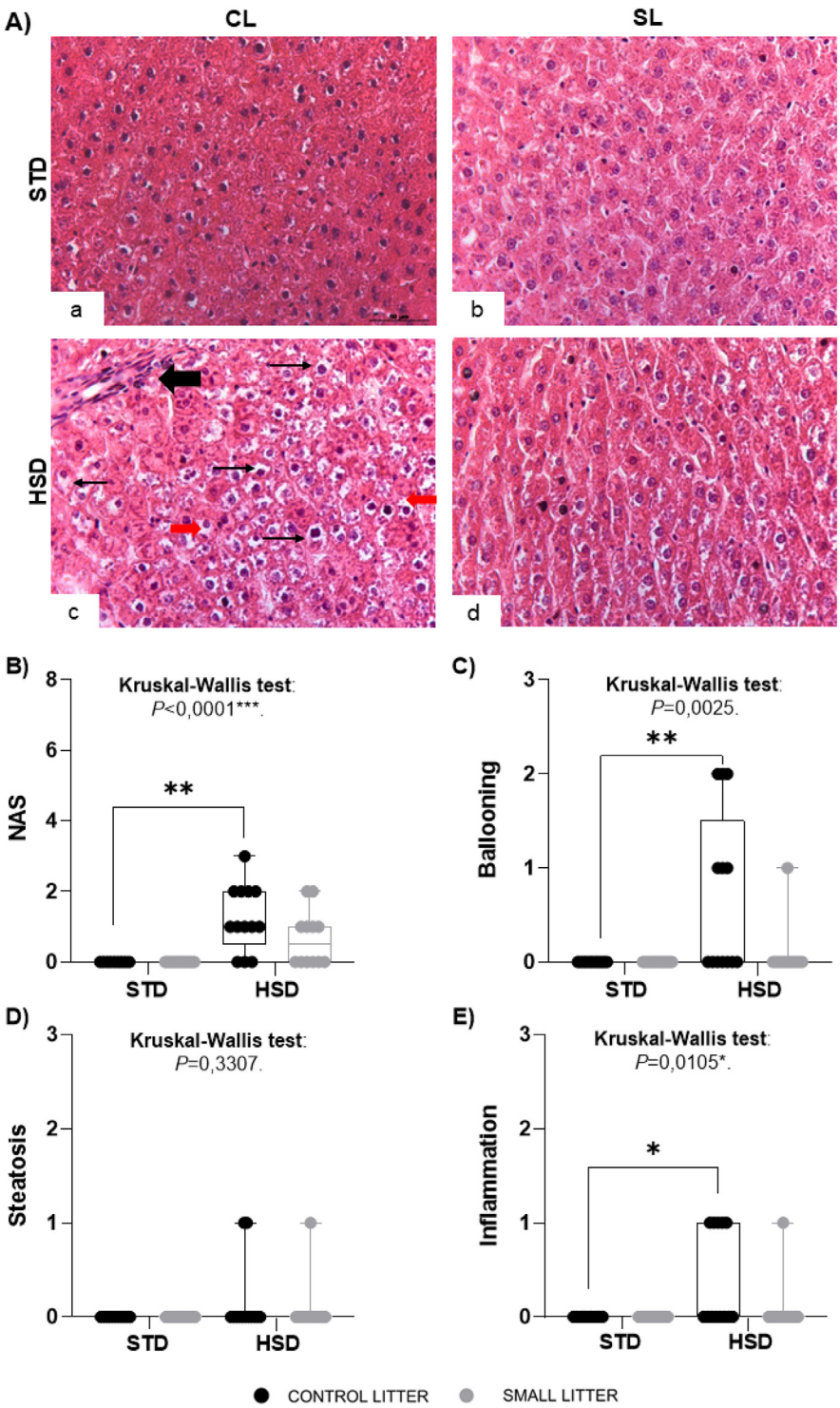

Fig. 2. SL mitigates hepatic histomorphological alterations induced by HSD after 8 weeks. (A) Representative histological sections of hepatocytes stained with hematoxylin-eosin (H&E) from each histological group (a: STD-CL; b: STD-SL; c: HSD-CL; d: HSD-SL). Thick arrows denote inflammatory infiltrates, thin arrows denote hepatocyte ballooning, and red arrows denote areas of macrovesicular steatosis. Scale bar=50 μm. Images were captured with a 40 × objective (field area of 215 × 161 μm^2) using a Leica DM5000B microscope with a digital camera. (B) NAS (STD-CL=11); (STD-SL=12); (HSD-CL=10); (HSD-SL=12); (C) Hepatocyte ballooning (STD-CL=11); (STD-SL=12); (HSD-CL=12); (HSD-SL=11); (D) Steatosis (STD-CL=11); (STD-SL=12); (HSD-CL=13); (HSD-SL=13); (E) Lobular inflammation (STD-CL=11); (STD-SL=12); (HSD-CL=12); (HSD-SL=11). Data normality was assessed using the Shapiro–Wilk test. Nonparametric data are presented as median with interquartile range (IQR) and are illustrated with box plots. Pups were analyzed individually as independent experimental units. Group comparisons were performed using the Kruskal–Wallis test with Dunn's *post hoc* test. CL, control litter; HSD, high-sucrose diet; IQR, interquartile range; NAS, nonalcoholic fatty liver disease activity score; SL, small litter; STD, standard diet. $^{*}P<.05$; $^{**}P<.01$; $^{***}P<.001$.

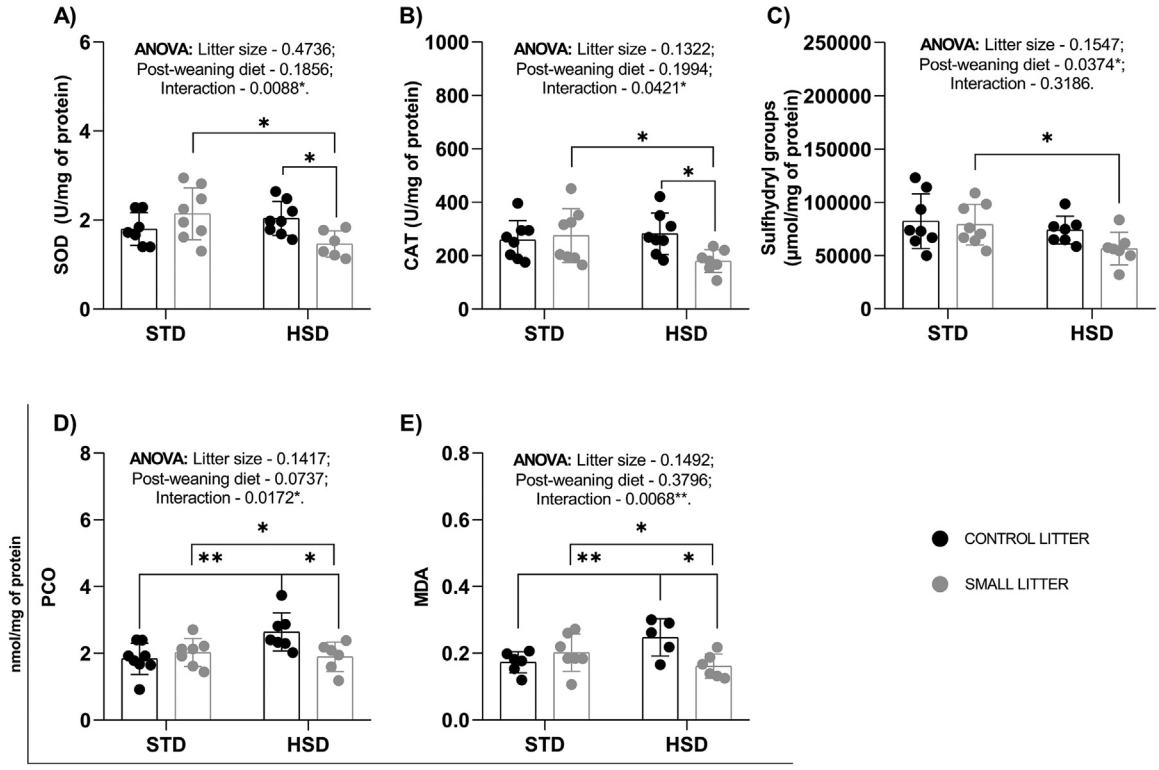

Fig. 3. SL attenuates hepatic oxidative damage induced by HSD after 8 weeks. A) Superoxide dismutase (SOD), U/mg protein (STD-CL=7); (STD-SL=8); (HSD-CL=8); (HSD-SL=6); B) Catalase (CAT), U/mg protein (STD-CL=8); (STD-SL=8); (HSD-CL=8); (HSD-SL=7); C) Sulfhydryl groups, µmol/mg protein (STD-CL=8); (STD-SL=8); (HSD-CL=7); (HSD-SL=7). D) Protein carbonyls (PCO), nmol/mg protein (STD-CL=8); (STD-SL=7); (HSD-CL=7); (HSD-SL=6); E) Malondialdehyde (MDA), nmol/mg protein (STD-CL=6); (STD-SL=7); (HSD-CL=5); (HSD-SL=6). Data normality was assessed using the Shapiro–Wilk test. Parametric data are represented as mean±SD and using bar graphs. Pups were analyzed individually as independent experimental units. The effects of litter size and post-weaning diet were assessed by two-way ANOVA, followed by the Bonferroni *post hoc* test. To evaluate the main effects independently (litter size and/or post-weaning diet), *post hoc* mean comparison tests were conducted when no interaction was observed. CL, control litter; STD, standard diet; HSD, high-sucrose diet; SL, small litter. $^{*}P<.05$; $^{**}P<.01$.

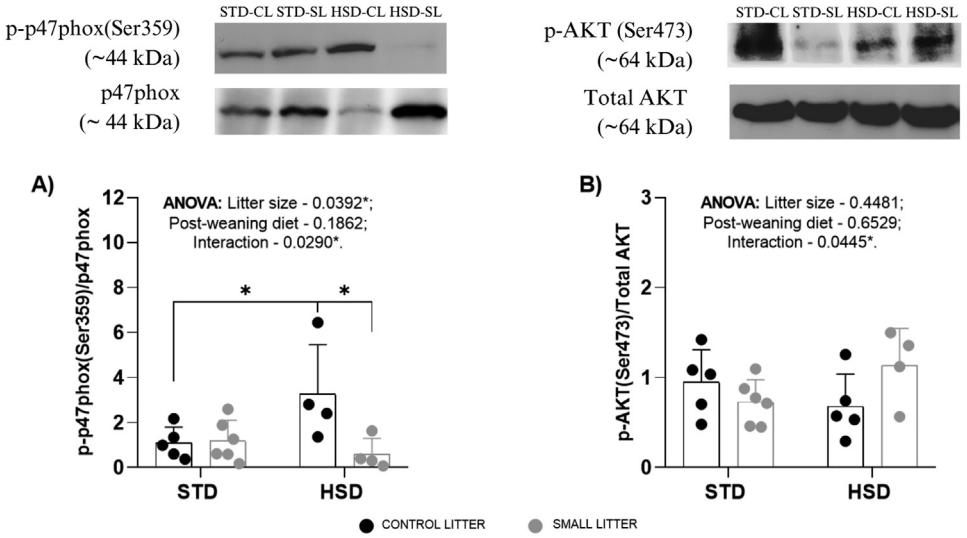

Fig. 4. SL mitigates p47phox (Ser359) phosphorylation induced by HSD associated with oxidative damage and reveals an interaction effect on p-AKT (Ser473) expression. (A) Protein expression of p-p47phox(Ser359)/p47phox (STD-CL=5); (STD-SL=6); (HSD-CL=4); (HSD-SL=4). (B) Protein expression of p-AKT(Ser473)/AKT (STD-CL=5); (STD-SL=6); (HSD-CL=5); (HSD-SL=4). Protein expression was normalized to total protein content assessed by Ponceau S staining after membrane transfer. Densitometric analyses included all biological replicates, whereas representative blots show one sample per group. Phosphorylated protein levels are expressed as the ratio of phosphorylated to total protein. Data normality was assessed using the Shapiro–Wilk test. Parametric data are represented as mean±SD and using bar graphs. Pups were analyzed individually as independent experimental units.The effects of litter size and post-weaning diet were assessed by two-way ANOVA, followed by the Bonferroni *post hoc* test. To evaluate the main effects independently (litter size and/or post-weaning diet), *post hoc* mean comparison tests were conducted when no interaction was observed. p-p47phox(Ser359), anti-phospho-p47phox (Ser359); p-AKT(Ser473), anti-phospho-AKT (Ser473); CL, control litter; HSD, high-sucrose diet; SL, small litter; STD, standard diet. $^{*}P<.05$; $^{**}P<.01$; $^{***}P<.001$.

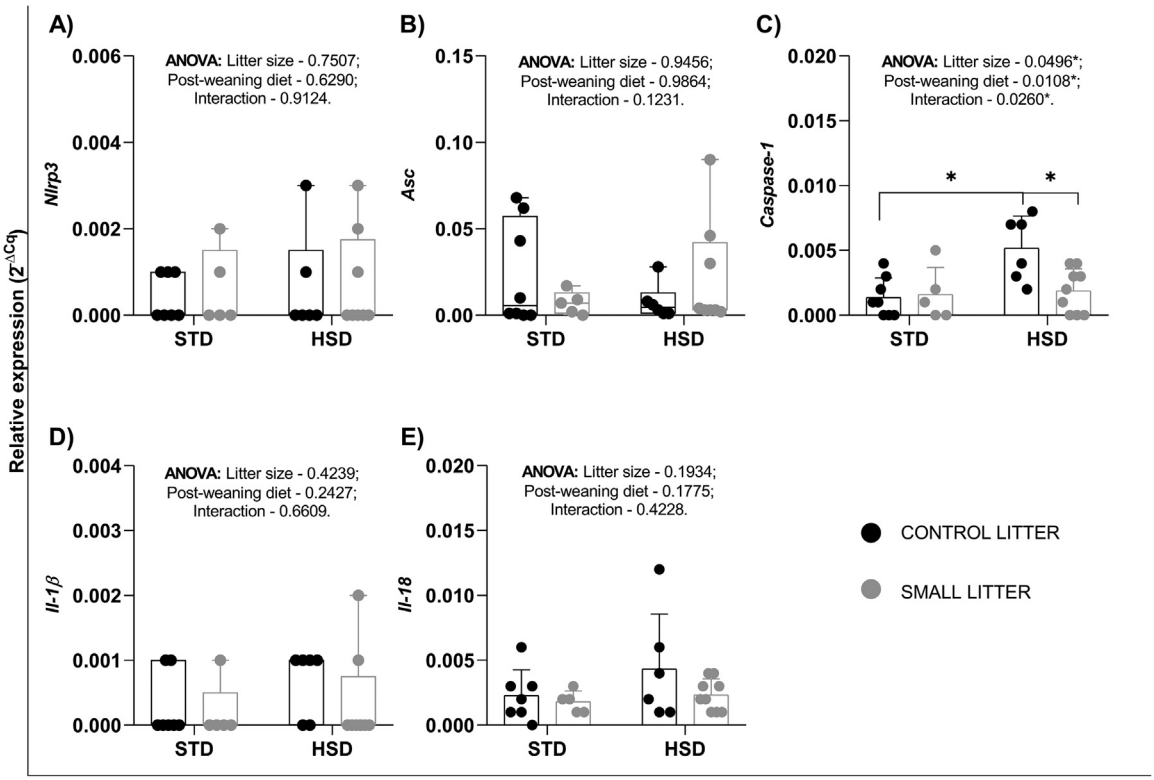

Fig. 5. SL attenuates *Caspase-1* upregulation induced by HSD within the hepatic NLRP3 inflammasome pathway. (A) *Nlrp3* (STD-CL=7); (STD-SL=5); (HSD-CL=6); (HSD-SL=8*);* (B) *Asc* (STD-CL=8); (STD-SL=5); (HSD-CL=6); (HSD-SL=8*);* C) *Caspase-1* (STD-CL=8); (STD-SL=5); (HSD-CL=6); (HSD-SL=9*);* D) *Il-1B* (STD-CL=7); (STD-SL=5); (HSD-CL=6); (HSD-SL=8*);* E) *Il-18* (STD-CL=7); (STD-SL=5); (HSD-CL=6); (HSD-SL=9). Expression profiles were assessed in the STD and HSD groups from 8 weeks of consumption using the $2^{-\Delta Cq}$ method. The relative gene expression of B2m was used as the reference gene. Data normality was assessed using the Shapiro–Wilk test. Parametric data are represented as mean±SD and using bar graphs, whereas nonparametric data are presented as median with interquartile range (IQR) and are illustrated with box plots. Pups were analyzed individually as independent experimental units. The effects of litter size and post-weaning diet were assessed by two-way ANOVA, followed by the Bonferroni *post hoc* test. To evaluate the main effects independently (litter size and/or post-weaning diet) *post hoc* mean comparison tests were conducted when no interaction was observed. *Asc*, apoptosis-associated speck-like protein containing a CARD domain; CL, control litter; HSD, high-sucrose diet; *Il-1B*, interleukin-1 beta; *Il-18*, interleukin-18; IQR, interquartile range; *Nlrp3*, NLR family pyrin domain-containing 3 receptor; STD, standard diet; SL, small litter. $^{*}P<0{,}05$.

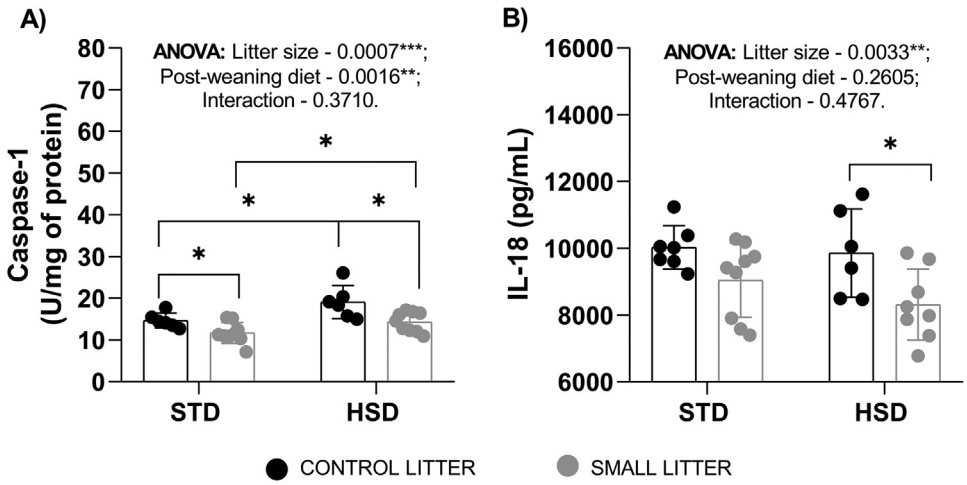

Fig. 6. SL attenuates caspase-1 activation induced by HSD and reduces IL-18 levels. (A) Caspase-1 activity in the liver; U/mg protein (STD-CL=6); (STD-SL=9); (HSD-CL=6); (HSD-SL=9). (B) Hepatic concentration of IL-18; pg/mL (STD-CL=7); (STD-SL=9); (HSD-CL=6); (HSD-SL=9). Data normality was assessed using the Shapiro–Wilk test. Parametric data are represented as mean±SD and using bar graphs. Pups were analyzed individually as independent experimental units. The effects of litter size and post-weaning diet were assessed by two-way ANOVA, followed by the Bonferroni *post hoc* test. To evaluate the main effects independently (litter size and/or post-weaning diet), *post hoc* mean comparison tests were conducted when no interaction was observed. CL, control litter; HSD, high-sucrose diet; SL, small litter; STD, standard diet. $^{*}P<.05$; $^{**}P<.01$; $^{***}P<.001$.

tively. Among the inflammasome-related genes, *Caspase-1* expression (Fig. 5C) was significantly influenced by litter size ($P<.05$), post-weaning diet ($P<.05$), and the interaction between variables ($P<.05$). The HSD-CL group exhibited a marked upregulation of *Caspase-1* (~270%) compared to the STD-CL group (0.0052±0.0025 *vs.* 0.0014±0.0015). Notably, this increase was significantly attenuated in the HSD-SL group (0.0019±0.0017), representing a reduction of ~60% relative to the HSD-CL group. IL-1β mRNA levels were not IL-1β mRNA levels were not consistently detectable in the majority of samples under the experimental conditions; therefore, protein expression analysis was not performed.

A similar pattern was observed in caspase-1 enzymatic activity (Fig. 6A), which was influenced by litter size ($P<.001$) and post-weaning diet ($P<.01$). The STD-SL (11.7±2.5) group showed a decrease of ~20% in caspase activity compared to STD-CL (14.66±1.76), whereas HSD-SL (14.33±2.36) showed an increase of 22% (compared to STD-SL). The HSD-CL group (19.12±3.97) exhibited a ~30% increase in activity compared to the STD-CL group. This increase was attenuated in the HSD-SL group (14.33±2.36), which presented values ~25% lower than HSD-CL. This enzymatic activity was directly reflected in hepatic IL-18 concentration (Fig. 6B), which was also modulated by litter size ($P<.01$). SL reduced IL-18 levels by a ~15.7% decrease in the HSD-SL group (8312±1063) compared to the HSD-CL group (9860±1322).

4. Discussion

Our study demonstrated that exposure to the SL model during early life may protect against liver injury induced by a post-weaning HSD in young rats. Although the harmful effects of excessive sucrose intake on hepatic health are well documented, our results suggest that SL may attenuate adverse hepatic changes induced by HSD, even in the presence of mild and heterogeneous steatotic alterations. This protective effect was reflected in NAS, hepatocellular ballooning, and inflammation, as the adverse effects of HSD observed in CL animals were mitigated in SL animals. Importantly, these findings should be interpreted within the context of a sucrose-enriched dietary pattern, reflecting a broader metabolic response to the dietary matrix rather than to isolated exposure to purified sucrose.

We suggest that the protective effects of SL are mechanistically linked to the attenuation of oxidative stress, as evidenced by the reduced phosphorylation of the NOX subunit p47phox (Ser359). We also observed reduced activation of the NLRP3 inflammasome, as indicated by decreased caspase-1 activity and lower hepatic IL-18 levels. Furthermore, hepatic p-AKT (Ser473) expression appeared to be modulated by the interaction between litter size and post-weaning diet, suggesting that early-life nutritional programming may shape hepatic insulin signaling responses to later dietary challenges, even in the absence of significant differences among individual groups.

In this study, we demonstrated liver injury induced by HSD in rats after 8 weeks, as evidenced by elevated ALT and AST levels. Despite no significant changes in relative liver mass, HSD consumption markedly increased hepatic lipid content, cholesterol, and TAG levels. These biochemical changes likely contribute to histological alterations such as hepatocellular ballooning and lobular inflammation, despite only mild and heterogeneous steatotic changes.

Our findings are consistent with previous reports showing that isocaloric diets rich in simple carbohydrates can lead to glucose intolerance and IR in Wistar rats [24,40,41]. Chronic HSD exposure (*e.g.*, 18 weeks) induces hepatic injury, alters the lipidome, and impairs fatty acid oxidation [42]. This process, driven by the activation of lipogenic transcription factors such as sterol regulatory element-binding protein 1c (SREBP-1c) and carbohydrate-responsive element-binding protein (ChREBP) [43–45], promotes hepatic TAG accumulation and elevates cholesterol levels, leading to histological changes, including ballooning and microvesicular steatosis, even in the absence of inflammation, as observed in Wistar male rats after 18 weeks of HSD [42]. Similar to our observations, Oliveira et al. [46] reported that 8 weeks of HSD in C57BL/6 male mice induced both macro- and microvesicular steatosis, along with increased inflammatory cytokines. Time-dependent changes in the hepatic morphology following sucrose exposure have consistently been linked to *de novo* lipogenesis [47,48]. Hepatocellular ballooning, which is frequently associated with oxidative stress, lipid accumulation, cytoskeletal disruption, and lipid peroxidation, is a key histological marker of hepatic injury [49,50]. In our study, elevated ALT and AST levels further supported hepatocyte damage after 8 weeks of HSD, helping to explain the underlying mechanism observed in the HSD-CL group [51].

Our results also show that early postnatal overnutrition induced by the SL model modulates MI and influences hepatic outcomes in response to post-weaning HSD. Most previous studies on heterogeneity agree that early life overnutrition affects liver metabolism, oxidative balance, and insulin sensitivity [16,20,52,53]. Notably, SL modifies milk composition and macronutrient content, with long-lasting effects on offspring metabolic trajectories [53,54].

Interestingly, in our study, SL alone increased the hepatic total cholesterol levels in standard chow-fed animals, which is consistent with previous reports [55]. However, SL did not increase the total lipid percentage or aminotransferase levels, and histological evaluation showed no changes in ballooning and inflammation. Although HSD increased these indices in CL animals, this effect was not evident in SL animals, suggesting that HSD-induced histological alterations were not observed. This pattern was consistent across both parametric and nonparametric analyses, even though interaction effects cannot be formally assessed using the latter. These findings suggest a protective or adaptive role of early life MI in mitigating diet-induced hepatic stress [24]. The varied outcomes across studies are likely related to differences in litter size, timing of assessments, and diet duration, underscoring the context-dependent nature of the SL effects [16]. Under the evaluated conditions, our results support a potential beneficial effect of early postnatal exposure to SLs in HSD-fed animals for 8 weeks.

Critical nutritional changes are closely associated with oxidative stress, a key contributor to metabolic dysfunctions such as IR and diabetes [56]. Diets rich in simple sugars, particularly sucrose, can promote ROS generation through NOX activation, thus exacerbating inflammation and IR progression [56,57]. In line with this, our previous work demonstrated that 8 weeks of HSD-induced IR and disrupted oxidative balance in muscles, reducing SOD activity and increasing PCO [40,41].

In the present study, HSD-CL animals exhibited a hepatic oxidative imbalance, as evidenced by increased MDA and PCO levels. This was concomitant with phosphorylation of the NOX subunit p47phox (Ser359), a modification known to enhance ROS production and promote lipid and protein oxidation [10,58]. This mechanism aligns with reports linking free fatty acid-induced ROS and PKCδ-mediated p47phox phosphorylation to proinflammatory signaling in IR, with NOX inhibition shown to mitigate this cycle [59].

Interestingly, HSD-SL animals displayed attenuated oxidative damage despite decreased sulfhydryl groups and slight reductions in SOD and CAT activities. Considering the complexity of redox regulation, we hypothesized that reduced ROS-driven NOX activation through p47phox phosphorylation contributes to this effect. This mechanism could be associated with the lower levels of oxidative damage markers observed in this group compared to the HSD-CL group. The diminished enzymatic activity may be partly explained

by reduced ROS production, and potentially by other regulatory mechanisms not assessed in this study, with alternative antioxidant pathways possibly involved [60].

These findings suggest that early life MI via SL modulates NOX activity and mitigates ROS-mediated injury, as reflected by the lower phosphorylated p47phox(Ser359) protein levels in the HSD-SL group. This protective effect contrasts with that of previous studies that reported SL-induced oxidative stress during early postnatal life (first 21 d), which reduced antioxidant enzyme activity and increased oxidative markers in young rats [20,21]. Together, these observations underscore the complex and context-dependent nature of the effect of SL on redox homeostasis, suggesting that the timing, duration, and nutritional context of SL exposure, as well as the compensatory adaptive mechanisms, critically determine whether SL promotes oxidative stress or confers protective effects later in life. Further studies are required to elucidate the precise molecular pathways and temporal dynamics underlying this dual effect.

One limitation of the present study was the use of the thiobarbituric acid-reacting substances assay; nevertheless, it remains widely employed for MDA quantification because of its methodological reproducibility and viability [8,32,60,61]. The lower NAS, reduced ballooning, and diminished inflammation observed in the HSD-SL group, along with the specific liver damage markers, support the hypothesis that the SL model may mitigate hepatic oxidative stress and injury induced by HSD. However, further studies are needed to confirm and clarify these protective effects.

Sustained hyperglycemia in Kupffer cells promotes lipid dysregulation and activates the NLRP3 inflammasome, partly through increased ROS production [62]. This process triggers the dissociation of TXNIP from TRX and consequently upregulates the expression of inflammatory genes in the liver [61–63]. NLRP3 inflammasome activation, a two-stage process, responds to hyperglycemia and oxidative stress, relying on the expression of *Nlrp3, Asc,* and *Caspase-1*, leading to the release of IL-1β and IL-18 [62,64,65]. Our previous results showed that HSD-CL animals exhibited systemic IR and increased oxidative damage, whereas SL attenuated these effects [24]. In the present study, HSD-CL livers showed elevated NOX expression, increased *Caspase-1* gene expression, and enzymatic activity, directly linking metabolic dysfunction to liver injury. In contrast, SL animals displayed reduced *Caspase-1* expression and activity in both the STD-SL and HSD-SL groups, which was accompanied by lower hepatic IL-18 levels in the HSD-SL animals. This suggests that early life MI via SL can modulate inflammasome activation and mitigate hepatic inflammation induced by HSD.

Only a few studies have investigated NLRP3 inflammasome activation in SL models. These studies have reported associations between SL and IR, noting increased NF-κB expression and NLRP3 activation and IL-1β, ultimately contributing to IRS1 phosphorylation at Ser307 and IR in female Wistar rats treated with 5α-dihydrotestosterone [66]. Similarly, NLRP3 activation associated with IR was observed in the hearts of C57BL/6 mice from SLs of three pups, potentially involving TXNIP upregulation [67]. Notably, these changes were not detected immediately after weaning, which highlights the importance of temporal assessments. Discrepancies across studies may be explained by differences in species, litter size, sex, tissue type, duration, and type of post-weaning intervention, and timing of analysis, all of which may have significant metabolic implications. Our findings indicate that both the timing and type of post-weaning intervention play a crucial role in the metabolic and inflammatory outcomes associated with SL in young adult Wistar rats fed an HSD for 8 weeks.

Importantly, increased proinflammatory cytokines contribute to cell pyroptosis and IR by disrupting the IRS/PI3K/AKT axis, including lower phosphorylation of AKT at Ser473 [14,68,69]. In a previous study, we demonstrated that SL protected HSD-fed animals from IR in the interscapular brown adipose tissue by upregulating p-AKT (Ser473) expression [24]. In the present study, SL altered p-AKT (Ser473) expression in the HSD-fed group, suggesting a modulatory effect on the insulin signaling pathway, although no statistically significant differences were detected in post hoc comparisons. Notably, within the STD-SL group, p-AKT (Ser473) expression was inversely correlated with p-p47phox (Ser359) phosphorylation ($R=-0.8857$, $P=.033$; data not shown). Although based on a limited within-group analysis, this observation may suggest an inverse association between redox-markers signaling and AKT activation, without implying causality. The phosphorylation of AKT at serine 473, mediated by mTORC2, plays a central role in hepatic insulin sensitivity [60,70,71]. In the context of early-life nutritional programming, the association observed in the STD-SL animals may reflect a modulation of hepatic insulin signaling by redox status. Nevertheless, further studies are warranted to clarify whether NOX activation directly influences AKT phosphorylation and its downstream pathways in this model.

To our knowledge, this study offers additional evidence indicating that MI induced by SL may attenuate adverse hepatic changes, including the modulation of pathways such as redox imbalance and NLRP3 inflammasome activation triggered by HSD exposure. Our findings indicate a complex interplay between hepatic morphological alterations, lipid accumulation, oxidative stress, NADPH oxidase activation via p47phox (Ser359) phosphorylation, and NLRP3 inflammasome activation, along with a global effect on p-AKT (Ser473) signaling. These findings suggest that the metabolic plasticity exerted by SL is more complex and context-dependent than previously reported, particularly in the context of post-weaning exposure to a deleterious diet. Overall, SL-induced MI may provide adaptive benefits in response to early-life dietary challenges, although these effects are nuanced and influenced by multiple factors.

5. Limitations of the study

Some limitations should be considered, including the inclusion of only male rats, which restricts extrapolation to females, in whom sex-specific differences in metabolism are well documented. Additionally, the variability of findings associated with litter size and the complexity of antioxidant pathways reinforce the need for future studies to include female animals in order to assess sex-specific responses to SL and HSD exposure, thereby enhancing our understanding of sexual dimorphism in early life MI. Another limitation of the present study is the absence of IL-1β protein quantification. Because *IL-1β* mRNA levels were not consistently detectable in the majority of samples under the experimental conditions, protein analysis was not pursued, and inflammasome-related outcomes were therefore assessed primarily through IL-18, which was selected due to its recognized immunometabolic relevance in hepatic tissue [72]. Finally, we acknowledge that our findings raise new questions and warrant further investigation, particularly regarding the elucidation of AKT downstream pathways and the metabolic responses arising from the interaction between SL and sucrose-enriched dietary intake.

6. Conclusion

In summary, these findings suggest that early life nutritional modulation through SL may beneficially influence metabolic outcomes in animals exposed to HSD. SL-induced MI appears to attenuate hepatic oxidative stress and inflammasome activation, which are hallmarks of diet-induced liver alterations, highlighting reductions in NOX p47phox(Ser359) expression, caspase-1 activity, and

IL-18 levels. These findings align with the DOHaD framework, suggesting that metabolic flexibility acquired early in life may offer resilience against nutritional insults later in development. Despite the limitations of this study and the need for further research, our results suggest that the SL is a valuable experimental model for exploring preventive strategies against metabolic dysfunction.

Glossary

AKT, protein kinase B; ALT, alanine aminotransferase; AST, aspartate aminotransferase; CAT, catalase; CL, control litter; DMSO, dimethyl sulfoxide; DOHaD, developmental origins of health and disease; HOMA-IR, homeostatic model assessment of insulin resistance; HSD, high-sucrose diet; IL-18, interleukin 18; IL-1β, interleukin 1 beta; IR, insulin resistance; IRS1, insulin receptor substrate 1; MASLD, metabolic dysfunction-associated steatotic liver disease; MDA, malondialdehyde; MI, metabolic imprinting; NAS, nonalcoholic fatty liver disease activity score; NLRP3, NOD-like receptor family pyrin domain-containing 3; NOX, NADPH oxidase; PCO, protein carbonyls; RIH, hepatic insulin resistance; ROS, reactive oxygen species; SL, small litter size; SOD, superoxide dismutase; STD, standard diet; TBARS - substances that react with thiobarbituric acid; TAG, triacylglycerol.

CRediT authorship contribution statement

Juliana Letícia Silva: Writing – review & editing, Writing – original draft, Visualization, Validation, Methodology, Investigation, Formal analysis, Data curation. **Isabela Jesus de Deus:** Writing – review & editing, Methodology, Investigation. **Aline Rezende Ribeiro de Abreu:** Writing – review & editing, Methodology, Investigation. **Miliane Martins de Andrade Fagundes:** Writing – review & editing, Methodology, Investigation. **Gustavo Silveira Breguez:** Writing – review & editing, Methodology, Investigation. **Cláudia Martins Carneiro:** Writing – review & editing, Resources, Methodology. **Sílvia Paula-Gomes:** Writing – review & editing, Resources, Methodology. **Daniela Caldeira Costa:** Writing – review & editing, Resources, Methodology. **Karina Barbosa de Queiroz:** Writing – review & editing, Writing – original draft, Visualization, Validation, Supervision, Project administration, Methodology, Investigation, Funding acquisition, Formal analysis, Conceptualization.

Acknowledgments

The authors thank the Animal Science Center (CCA/UFOP) for animal care and housing, and acknowledge the support of FINEP, FAPEMIG (APQ-02200-21, APQ-02029-21, APQ-04983-22, APQ-02511-22), CAPES, and CNPq. We are also grateful to the Multiuser Laboratory for Advanced Microscopy and Microanalysis (LMU-MAM/NUPEB/UFOP) and the Cipharma Multiuser Laboratory (LM1) for technical support, and to Eduarda dos Santos and Melina Oliveira de Souza for contributions; Raphael Antônio Borges Gomes, Luciana da Fonseca Medeiros, Rosália da Conceição Alves Lopes, Nívia Carolina Nogueira de Paiva, Rosana da Conceição Araújo Maia and Sttefany Viana Gomes for their assistance with the experiments.

Declaration of competing interest

The authors declare the following financial interests/personal relationships which may be considered as potential competing interests: Karina Barbosa de Queiroz reports was provided by Minas Gerais State Foundation of Support to the Research. If there are other authors, they declare that they have no known competing financial interests or personal relationships that could have appeared to influence the work reported in this paper.

Funding

This work has financial support from the Postgraduate Development Program (PDPGIII), the Minas Gerais State Research Foundation (FAPEMIG - APQ - 04983-22), and the Coordination for the Improvement of Higher Education Personnel (CAPES).

Supplementary materials

Supplementary material associated with this article can be found, in the online version, at doi:10.1016/j.jnutbio.2026.110372.

References

[1] Lucas A. Role of nutritional programming in determining adult morbidity. Arch Dis Child 1994;71:288. doi:10.1136/ADC.71.4.288.
[2] Monk D, Mackay DJG, Eggermann T, Maher ER, Riccio A. Genomic imprinting disorders: lessons on how genome, epigenome and environment interact. Nat Rev Genet 2019;20:235–48. doi:10.1038/s41576-018-0092-0.
[3] Barker DJP. The fetal and infant origins of adult disease. BMJ : Br Med J 1990;301:1111. doi:10.1136/BMJ.301.6761.1111.
[4] Penkler M, Hanson M, Biesma R, Müller R. DOHaD in science and society: emergent opportunities and novel responsibilities. J Dev Orig Health Dis 2019;10:268–73. doi:10.1017/S2040174418000892.
[5] WHO Guideline: Sugars intake for adults and children, Geneva: World Health Organization; 2015. ISBN-13: 978-92-4-154902-8.
[6] Vos MB, Kaar JL, Welsh JA, Van Horn L V, Feig DI, Anderson CAM, et al. Added sugars and cardiovascular disease risk in children: a scientific statement from the American Heart Association. Circulation 2017;135:e1017–34. doi:10.1161/CIR.0000000000000439.
[7] Wu Y, Tan Z, Zhen J, Liu C, Zhang J, Liao F, et al. Association between diet soft drink consumption and metabolic dysfunction-associated steatotic liver disease: findings from the NHANES. BMC Public Health 2023;23. doi:10.1186/S12889-023-17223-0.
[8] Acosta-Cota S de J, Aguilar-Medina EM, Ramos-Payán R, Ruiz-Quiñónez AK, Romero-Quintana JG, Montes-Avila J, et al. Histopathological and biochemical changes in the development of nonalcoholic fatty liver disease induced by high-sucrose diet at different times. Can J Physiol Pharmacol 2019;97:23–36. doi:10.1139/CJPP-2018-0353.
[9] Sigma SHA. The effect and mechanism of sucrose consumption to liver disease – a systematic literature review. Biomol Health Sci J 2022;5:47–53. doi:10.20473/BHSJ.V5I1.35160.
[10] Babior BM. NADPH oxidase: an update. Blood 1999;93:1464–76. doi:10.1182/BLOOD.V93.5.1464.
[11] Brieger K, Schiavone S, Miller FJ, Krause KH. Reactive oxygen species: from health to disease. Swiss Med Wkly 2012;33:142. doi:10.4414/SMW.2012.13659.
[12] Hotamisligil GS. Inflammation, metaflammation and immunometabolic disorders. Nature 2017;542:177–85. doi:10.1038/NATURE21363.
[13] Broz P, Dixit VM. Inflammasomes: mechanism of assembly, regulation and signalling. Nat Rev Immunol 2016;16:407–20. doi:10.1038/nri.2016.58.
[14] Jia X, Qiu T, Yao X, Jiang L, Wang N, Wei S, et al. Arsenic induces hepatic insulin resistance via mtROS-NLRP3 inflammasome pathway. J Hazard Mater 2020;399:123034. doi:10.1016/J.JHAZMAT.2020.123034.
[15] Spencer SJ. Perinatal nutrition programs neuroimmune function long-term: mechanisms and implications. Front Neurosci 2013;7:47983. doi:10.3389/FNINS.2013.00144/BIBTEX.
[16] Parra-Vargas M, Ramon-Krauel M, Lerin C, Jimenez-Chillaron JC. Size does matter: litter size strongly determines adult metabolism in rodents. Cell Metab 2020;32:334–40. doi:10.1016/j.cmet.2020.07.014.
[17] Plagemann A, Heidrich I, Götz F, Rohde W, Dörner G. Obesity and enhanced diabetes and cardiovascular risk in adult rats due to early postnatal overfeeding. Exp Clin Endocrinol Diabetes 1992;99:154–8. doi:10.1055/S-0029-1211159/BIB.
[18] Cai G, Dinan T, Barwood JM, De Luca SN, Soch A, Ziko I, et al. Neonatal overfeeding attenuates acute central pro-inflammatory effects of short-term high fat diet. Front Neurosci 2015;9. doi:10.3389/fnins.2014.00446.
[19] Cassiano LMG, de Queiroz KB, Martins TV de A, Maia ALA, Rachid MA, Spencer SJ, et al. Neonatal overfeeding attenuates microgliosis and hippocampal damage in an infant rat model of pneumococcal meningitis. Front Immunol 2024;15. doi:10.3389/FIMMU.2024.1429157.
[20] Conceição EPS, Franco JG, Oliveira E, Resende AC, Amaral TAS, Peixoto-Silva N, et al. Oxidative stress programming in a rat model of postnatal early overnutrition - role of insulin resistance. J NutrBiochem 2013;24:81–7. doi:10.1016/j.jnutbio.2012.02.010.
[21] Conceição EPS, Moura EG, Carvalho JC, Oliveira E, Lisboa PC. Early redox imbalance is associated with liver dysfunction at weaning in overfed rats. J Physiol 2015;593:4799. doi:10.1113/JP271189.

[22] Zhang X, Zhang JH, Chen XY, Hu QH, Wang MX, Jin R, et al. Reactive oxygen species-induced TXNIP Drives fructose-mediated hepatic inflammation and lipid accumulation through NLRP3 inflammasome activation. Antioxid Redox Signal 2015;22:848–70. doi:10.1089/ARS.2014.5868.
[23] Veličković N, Teofilović A, Ilić D, Djordjevic A, Vojnović Milutinović D, Petrović S, et al. Modulation of hepatic inflammation and energy-sensing pathways in the rat liver by high-fructose diet and chronic stress. Eur J Nutr 2019;58:1829–45. doi:10.1007/S00394-018-1730-1.
[24] de Deus IJ, de Abreu ARR, Fagundes MM de A, Silva JL, Breguez GS, Silva ÂA, et al. Metabolic imprinting due to small litter size mitigates insulin resistance through the interscapular brown adipose tissue activation in a high-sucrose diet model. J Dev Orig Health Dis 2025;16:e29. doi:10.1017/S2040174425100123.
[25] Spencer SJ, Tilbrook A. Neonatal overfeeding alters adult anxiety and stress responsiveness. Psychoneuroendocrinology 2009;34:1133–43. doi:10.1016/j.psyneuen.2009.02.013.
[26] Sengupta P. The laboratory rat: relating its age with human's. Int J Prev Med 2013;4:624.
[27] Maharani NPR, Fadlyah NA, Setyaningrum DAW, Hairunisa N. Effects of euthanasia on animal research. Ve Biomed Clin J 2024;6:41–6. doi:10.21776/ub.VetBioClinJ.2024.006.01.6.
[28] Folch J, Lees M, Sloane GH. A simple method for the isolation and purification of total lipides from animal tissues*. J Biol Chem 1957;226:497–509. doi:10.1016/S0021-9258(18)64849-5.
[29] Kleiner DE, Brunt EM, Van Natta M, Behling C, Contos MJ, Cummings OW, et al. Design and validation of a histological scoring system for nonalcoholic fatty liver disease. Hepatology 2005;41:1313–21. doi:10.1002/HEP.20701.
[30] Peng C, Stewart AG, Woodman OL, Ritchie RH, Qin CX. Non-alcoholic steatohepatitis: a review of its mechanism, models and medical treatments. Front Pharmacol 2020;11:603926. doi:10.3389/FPHAR.2020.603926/BIBTEX.
[31] Lowry O, Rosebrough N, Farr A, Randall R. Protein measurement with the Folin phenol reagent. J Biol Chem 1951;193:265–75.
[32] Conceição EPS, Moura EG, Oliveira E, Guarda DS, Figueiredo MS, Quitete FT, et al. Dietary calcium supplementation in adult rats reverts brown adipose tissue dysfunction programmed by postnatal early overfeeding. J Nutr Biochem 2017;39:117–25. doi:10.1016/j.jnutbio.2016.09.013.
[33] Madesh M, Balasubramanian KA. Microtiter plate assay for superoxide dismutase using MTT reduction by superoxide. Indian J Biochem Biophys 1998;35:184–8.
[34] Aebi H. Catalase in vitro. Methods Enzymol 1984;105:121–6. doi:10.1016/S0076-6879(84)05016-3.
[35] Sedlak J, Lindsay RH. Estimation of total, protein-bound, and nonprotein sulfhydryl groups in tissue with Ellman's reagent. Anal Biochem 1968;25:192–205. doi:10.1016/0003-2697(68)90092-4.
[36] Levine RL, Williams JA, Stadtman EP, Shacter E. Carbonyl assays for determination of oxidatively modified proteins. Methods Enzymol 1994;233:346–57. doi:10.1016/S0076-6879(94)33040-9.
[37] Buege JA, Aust SD. Microsomal lipid peroxidation. Methods Enzymol 1978;52:302–10. doi:10.1016/S0076-6879(78)52032-6.
[38] Sander H, Wallace S, Plouse R, Tiwari S, Gomes AV. Ponceau S waste: Ponceau S staining for total protein normalization. Anal Biochem 2019;575:44–53. doi:10.1016/j.ab.2019.03.010.
[39] Silver N, Best S, Jiang J, Thein SL. Selection of housekeeping genes for gene expression studies in human reticulocytes using real-time PCR. BMC Mol Biol 2006;7:1–9. doi:10.1186/1471-2199-7-33/FIGURES/3.
[40] de Queiroz KB, Guimarães JB, Coimbra CC, Rodovalho GV, Carneiro CM, Evangelista EA, et al. Endurance training increases leptin expression in the retroperitoneal adipose tissue of rats fed with a high-sugar diet. Lipids 2014;49:85–96. doi:10.1007/s11745-013-3854-7.
[41] de Queiroz KB, Honorato-Sampaio K, Júnior JVR, Leal DA, Pinto ABG, Kappes-Becker L, et al. Physical activity prevents alterations in mitochondrial ultrastructure and glucometabolic parameters in a high-sugar diet model. PLoS One 2017;12. doi:10.1371/journal.pone.0172103.
[42] Oliveira DT, Chaves-Filho AB, Yoshinaga MY, Paiva NCN, Carneiro CM, Miyamoto S, et al. Liver lipidome signature and metabolic pathways in non-alcoholic fatty liver disease induced by a high-sugar diet. J Nutr Biochem 2021;87:108519. doi:10.1016/J.JNUTBIO.2020.108519.
[43] Alves-Bezerra M, Cohen DE. Triglyceride metabolism in the liver. Compr Physiol 2017;8:1. doi:10.1002/CPHY.C170012.
[44] Sanders FWB, Griffin JL. De novo lipogenesis in the liver in health and disease: more than just a shunting yard for glucose. Biol Rev Camb Philos Soc 2016;91:452. doi:10.1111/BRV.12178.
[45] Softic S, Cohen DE, Kahn CR. Role of dietary fructose and hepatic de novo lipogenesis in fatty liver disease. Dig Dis Sci 2016;61:1282. doi:10.1007/S10620-016-4054-0.
[46] Oliveira LSC, Santos DA, Barbosa-da-Silva S, Mandarim-de-Lacerda CA, Aguila MB. The inflammatory profile and liver damage of a sucrose-rich diet in mice. J Nutr Biochem 2014;25:193–200. doi:10.1016/J.JNUTBIO.2013.10.006.
[47] de Oliveira DT, Fernandes I da C, de Sousa GG, Dos Santos TAP, de Paiva NCN, Carneiro CM, et al. High-sugar diet leads to obesity and metabolic diseases in ad libitum -fed rats irrespective of caloric intake. Arch Endocrinol Metab 2020;64:71–81. doi:10.20945/2359-3997000000199.
[48] Plazas Guerrero CG, Acosta Cota SDJ, Castro Sánchez FH, Vergara Jiménez MDJ, Ríos Burgueño ER, Sarmiento Sánchez JI, et al. Evaluation of sucrose-enriched diet consumption in the development of risk factors associated to type 2 diabetes, atherosclerosis and non-alcoholic fatty liver disease in a murine model. Int J Environ Health Res 2021;31:651–69. doi:10.1080/09603123.2019.1680817.
[49] Celebi G, Cicek AF, Gurel H, Genc H, Kirik A, Ercin CN, et al. Microvesicular steatosis : a missed item in the management of nonalcoholic fatty liver disease? Acta Gastroenterol Belg 2020;83:565–70.
[50] Mitten EK, Baffy G. Mechanotransduction in the pathogenesis of non-alcoholic fatty liver disease. J Hepatol 2022;77:1642–56. doi:10.1016/J.JHEP.2022.08.028/ATTACHMENT/DD85A0F2-C7A8-4825-89B1-01E5B1265E08/MMC1.PDF.
[51] Sanal MG. Biomarkers in nonalcoholic fatty liver disease-the emperor has no clothes? World J Gastroenterol 2015;21:3223–31. doi:10.3748/wjg.v21.i11.3223.
[52] Dorner G, Plagemann A. Perinatal hyperinsulinism as possible predisposing factor for diabetes mellitus, obesity and enhanced cardiovascular risk in later life. Hormone Metab Res 1994;26:213–21. doi:10.1055/s-2007-1001668.
[53] Ramon-Krauel M, Pentinat T, Bloks VW, Cebrià J, Ribo S, Pérez-Wienese R, et al. Epigenetic programming at the Mogat1 locus may link neonatal overnutrition with long-term hepatic steatosis and insulin resistance. FASEB J 2018;32:6025–37. doi:10.1096/FJ.201700717RR.
[54] Xavier JLP, Scomparin DX, Pontes CC, Ribeiro PR, Cordeiro MM, Marcondes JA, et al. Litter size reduction induces metabolic and histological adjustments in dams throughout lactation with early effects on offspring. An Acad Bras Cienc 2019;91. doi:10.1590/0001-3765201920170971.
[55] Rinaldi W, Ribeiro TA, da S, Marques AS, Fabricio GS, Tófolo LP, et al. Efeito da redução de ninhada sobre as respostas autonômicas e metabólicas de ratos Wistar. Rev Nutr 2012;25:321–30. doi:10.1590/S1415-52732012000300002.
[56] Tan BL, Norhaizan ME, Liew WPP. Nutrients and oxidative stress: friend or foe? Oxid Med Cell Longev 2018;2018. doi:10.1155/2018/9719584.
[57] de SDJM, de SLLC, Rodrigues JR, Learte LRS, dos SGM. Influência do índice glicêmico dos alimentos sobre a concentração de marcadores pró-inflamatórios. Arch Health Investig 2020;9:2020. doi:10.21270/ARCHI.V9I1.3220.
[58] Begum R, Thota S, Abdulkadir A, Kaur G, Bagam P, Batra S. NADPH oxidase family proteins: signaling dynamics to disease management. Cell Mol Immunol 2022;19:660. doi:10.1038/S41423-022-00858-1.
[59] Pereira S, Park E, Mori Y, Andrew Haber C, Han P, Uchida T, et al. FFA-induced hepatic insulin resistance in vivo is mediated by PKCδ, NADPH oxidase, and oxidative stress. Am J Physiol Endocrinol Metab 2014;307:E34. doi:10.1152/AJPENDO.00436.2013.
[60] Bandeira SDM, Guedes GDS, Fonseca LJSD, Pires AS, Gelain DP, Moreira JCF, et al. Characterization of blood oxidative stress in type 2 diabetes mellitus patients: increase in lipid peroxidation and SOD Activity. Oxid Med Cell Longev 2012;2012:13. doi:10.1155/2012/819310.
[61] Rolnik A, Olas B, Szablińska-Piernik J, Lahuta LB, Gromadziński L, Majewski MS. Antioxidant and anticoagulant properties of myo-inositol determined in an ex vivo studies and gas chromatography analysis. Sci Rep 2024;14:1–13. doi:10.1038/s41598-024-76527-2.
[62] Zheng T, Wang Q, Dong Y, Ma W, Zhang Y, Zhao Y, et al. High glucose-aggravated hepatic insulin resistance: role of the NLRP3 Inflammasome in Kupffer cells. Obesity 2020;28:1270–82. doi:10.1002/OBY.22821.
[63] Russell-Guzmán J, Américo-Da Silva L, Cadagan C, Maturana M, Palomero J, Estrada M, et al. Activation of the ROS/TXNIP/NLRP3 pathway disrupts insulin-dependent glucose uptake in skeletal muscle of insulin-resistant obese mice. Free Radic Biol Med 2024;222:187–98. doi:10.1016/j.freeradbiomed.2024.06.011.
[64] Haneklaus M, O'Neill LAJ. NLRP3 at the interface of metabolism and inflammation. Immunol Rev 2015;265:53–62. doi:10.1111/IMR.12285.
[65] Ma Q. Pharmacological Inhibition of the NLRP3 Inflammasome: structure, molecular activation, and inhibitor-NLRP3 interaction. Pharmacol Rev 2023;75:487. doi:10.1124/PHARMREV.122.000629.
[66] Veličković N, Mićić B, Teofilović A, Milovanovic M, Jovanović M, Djordjevic A, et al. Overfeeding in the early postnatal period aggravates inflammation and hepatic insulin sensitivity in the 5α-dihydrotestosterone-induced animal model of PCOS. Front Endocrinol (Lausanne) 2024;15:1402905. doi:10.3389/FENDO.2024.1402905.
[67] Siddeek B, Li N, Mauduit C, Chehade H, Rigal E, Tolsa JF, et al. Transient postnatal over nutrition induces long-term alterations in cardiac NLRP3-inflammasome pathway. Nutr Metab Cardiovasc Dis 2018;28:944–51. doi:10.1016/j.numecd.2018.03.013.
[68] Marín-Aguilar F, Lechuga-Vieco AV, Alcocer-Gómez E, Castejón-Vega B, Lucas J, Garrido C, et al. NLRP3 inflammasome suppression improves longevity and prevents cardiac aging in male mice. Aging Cell 2020;19:13050. doi:10.1111/ACEL.13050.
[69] Rheinheimer J, de Souza BM, Cardoso NS, Bauer AC, Crispim D. Current role of the NLRP3 inflammasome on obesity and insulin resistance: a systematic review. Metabolism 2017;74:1–9. doi:10.1016/j.metabol.2017.06.002.
[70] Saltiel AR. Insulin signaling in health and disease. J Clin Invest 2021;131. doi:10.1172/JCI142241.
[71] Petersen MC, Shulman GI. Mechanisms of insulin action and insulin resistance. Physiol Rev 2018;98:2133. doi:10.1152/PHYSREV.00063.2017.
[72] Somm E, Jornayvaz FR. Interleukin-18 in metabolism: from mice physiology to human diseases. Front Endocrinol (Lausanne) 2022;13:971745. doi:10.3389/fendo.2022.971745.